DOI: 10.61782/fa.2023.0842

forum acusticum 2023

MAXIMUM DIRECTIVITY OF FLANGED OPEN-ENDED WAVEGUIDES

Hao Dong[1*] **Jean-Baptiste Doc**[2] **Simon Félix**[1]

[1] Laboratoire d'Acoustique de l'Université du Mans (LAUM), UMR 6613, Institut d'Acoustique Graduate School (IA-GS), CNRS, 72085 Le Mans, France
[2] Laboratoire de Mécanique des Structures et des Systèmes Couplés, Conservatoire National des Arts et Métiers, 75003 Paris, France

ABSTRACT

Directional beams have broad applications in communication and sound reproduction. This paper investigates the theoretical maximum directivity of an infinitely flanged aperture of arbitrary cross-section by means of modal decomposition. We derive a rigorous, algebraic, global maximum solution of the directivity factor, by which a directional beam in a desired direction can be created. Assuming the aperture as the opening of a waveguide, we construct a group of incident modes or a point-source array within the waveguide for synthesizing the theoretical beam obtained in a subspace spanned by all the propagating modes. We elucidate that when the evanescent modes are included in the maximization, the maximum directivity factor increases with considerable loss to the radiation efficiency. Nevertheless, in some cases, the optimum aperture velocity dominated by the lowest-order evanescent components could still be useful for designing metamaterial-lens horn antennas.

Keywords: *directional acoustic radiation*, *maximum directivity*, *open-ended waveguide*, *radiation pattern synthesis*, *acoustic horn antenna*

1. INTRODUCTION

The directivity factor is a common metric to measure the directivity from a source. Thus, directional beams can be designed by performing design optimization with respect to it. Apart from using numerical optimization algorithms, rigorous and closed-form solutions of the maximum directivity factor have been studied for acoustic line source arrays [1] and spherical arrays [2]. Acoustic waveguides with super-directivity are of great practical significance. However, the theoretical maximum directivity factor from waveguides is still an open question. In this work, we investigate the maximum directivity of an infinitely flanged aperture using modal expansion of the aperture velocity, and then study the directivity pattern synthesis.

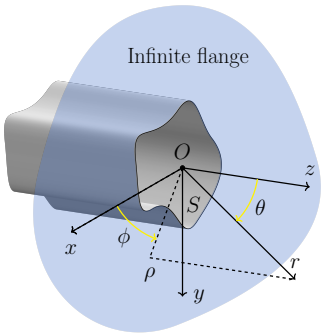

Figure 1. Coordinate system for a flanged aperture S. The radius vector $\boldsymbol{r}$ is given by (x, y, z) or (r, θ, ϕ).

2. MAXIMUM DIRECTIVITY FACTOR AND OPTIMAL BEAM PATTERN

Consider an aperture of arbitrary shape opened on an infinite rigid baffle, as shown in Fig. 1. The far-field directiv-

*__Corresponding author__: hao.dong@univ-lemans.fr.

ity function can be expressed by the z component of the aperture velocity [3]:

$$D(\theta,\phi) = \frac{1}{2\pi}\iint_S v_z\,(x,y,0)\,\mathrm{e}^{-\mathrm{i}(k_x x + k_y y)}\mathrm{d}x\mathrm{d}y, \quad (1)$$

where $k_x = k\sin\theta\cos\phi$ and $k_y = k\sin\theta\sin\phi$. To couple the radiated field with the propagation within the waveguide, the velocity is projected onto the rigid waveguide modes (eigenmodes of the transverse Laplacian with Neumann boundary condition), $v_z(x,y,0) = \sum_{n=0}^{\infty} v_n\varphi_n(x,y)$. Substituting this modal expansion into Eq. (1) yields $D(\theta,\phi) = \sum_{n=0}^{\infty} v_n\Upsilon_n(\theta,\phi)$, where Υ_n is the modal directivity function.

The directivity factor is defined as the ratio of the intensity I_r in a specified direction to the intensity that would be produced at the same position by a point source radiating the same power W [4]:

$$Q(\theta,\phi) = \frac{I_r(r,\theta,\phi)}{W/2\pi r^2}, \quad (2)$$

which can be rewritten in a matrix form:

$$Q(\theta,\phi) = 2\pi\frac{\mathbf{v}^\dagger \mathsf{A}^*(\theta,\phi)\mathbf{v}}{\mathbf{v}^\dagger \mathsf{C}\mathbf{v}}, \quad (3)$$

where $\mathsf{A} = \boldsymbol{\Upsilon}\boldsymbol{\Upsilon}^\dagger$ is Hermitian and of rank one, and the coupling matrix

$$\mathsf{C} = \int_0^{2\pi}\mathrm{d}\phi\int_0^{\pi/2}\boldsymbol{\Upsilon}\boldsymbol{\Upsilon}^\dagger\sin\theta\mathrm{d}\theta \quad (4)$$

is Hermitian, positive definite, real, and non-singular. The properties of matrices A and C guarantee that Eq. (3) is a generalized Rayleigh quotient [5]. Therefore, Q has a global maximum $Q_{\max}$ that is equal to $2\pi\lambda_{\max}$, where $\lambda_{\max}$ is the largest eigenvalue of the generalized eigenvalue problem

$$\mathsf{A}^*\mathbf{v} = \lambda\mathsf{C}\mathbf{v}, \quad (5)$$

and the eigenvector $\mathbf{v}_{\mathrm{opt}}$ corresponding to $\lambda_{\max}$ represents the optimum aperture velocity function $v_{\mathrm{opt}}(x,y) = \mathbf{v}_{\mathrm{opt}}^{\mathrm{T}}\boldsymbol{\varphi}(x,y)$. Besides, Eq. (5) has only one positive eigenvalue.

Solving the optimum velocity in the complete space of square-integrable functions necessitates the incorporation of an infinite number of modes. It is reasonable to consider the subspace consisting of all propagating modes (eigenvalues $\gamma_n \le k$) at a given frequency. The following is a case study of the maximum directivity for a typical circular aperture.

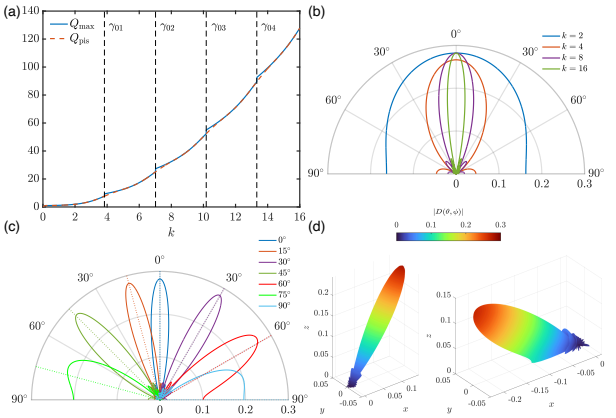

Figure 2. (a) Comparison of $Q_{\max}(0)$ and Q_{pis}. (b) Optimum patterns for $\theta_{\mathrm{d}} = 0°$ in the xz plane at several frequencies. (c) Optimum directivity patterns in the xz plane at $k = 16$ for different target directions marked with dotted lines. (d) Three-dimensional optimal beam patterns steered in directions $(30°, 0°)$ and $(60°, 180°)$ at $k = 16$.

First, the axial directivity factor (target angle $\theta_{\mathrm{d}} = 0°$) is maximized in the propagating modal subspace. It is then compared with the directivity factor of a vibrating piston. As shown in Fig. 2(a), the piston mode is a reasonable guess for the optimum velocity. The optimum directivity patterns are shown in Fig. 2(b). Figs. 2(c) and 2(d) show off-axis optimal beams. For small off-axis angles, the beam is steered precisely to the desired direction, and its main lobe exhibits good symmetry. However, near the sideline directions, the main lobe slightly deviates from the target angle and exhibits degraded symmetry.

3. BEAM PATTERN SYNTHESIS

3.1 Multimodal incidence

The theoretical optimal beams can be synthesized by a group of incident modes. They are determined such that the propagating components of the aperture velocity are identical to v_{opt}. Given the incident pressure field $\mathbf{p}_+$ at the output ($z = 0$), the total velocity field is

$$\begin{bmatrix}\mathbf{v}_{\mathrm{opt}}\\ \mathbf{v}_{\mathrm{e}}\end{bmatrix} = \mathsf{Y}_{\mathrm{c}}\,(\mathsf{I}-\mathsf{R})\,\mathbf{p}_+, \quad (6)$$

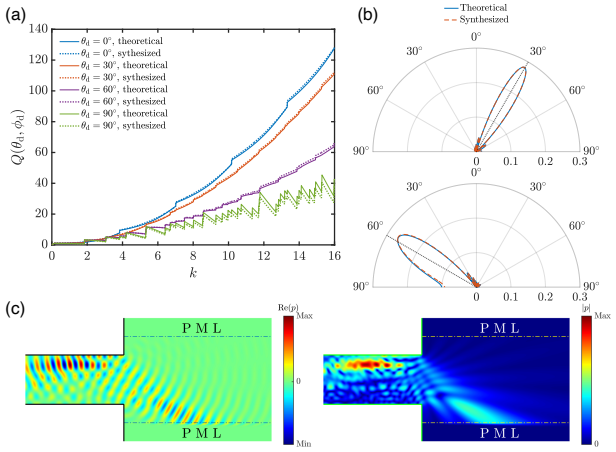

Figure 3. (a) Comparison of $Q_{\max}$ and Q_{syn}. (b) Comparison of the theoretical and synthesized patterns for $(30°, 0°)$ and $(60°, 180°)$ at $k = 16$ in xz plane [corresponding to Fig. 2(c)]. (c) Real part (left) and magnitude (right) of the pressure field in the xz plane generated by incident propagating modes for the directivity synthesis in $(30°, 0°)$ at $k = 16$, computed by the PML-multimodal method [6].

where Y_c is the characteristic admittance matrix, which is diagonal with elements $\sqrt{k^2 - \gamma_n^2}/k$,

$$\mathsf{R} = (\mathsf{I} + \mathsf{Z}_\text{r}\mathsf{Y}_\text{c})^{-1}(\mathsf{Z}_\text{r}\mathsf{Y}_\text{c} - \mathsf{I}) \tag{7}$$

is the reflection matrix, Z_r is the radiation impedance matrix, and $\mathbf{v}_\text{e}$ is the evanescent velocity field (truncated at length N_e for computation). By blocking matrices Y_c and $(\mathsf{I}-\mathsf{R})$ according to the dimensions of $\mathbf{v}_\text{opt}$ and $\mathbf{v}_\text{e}$, Eq. (6) can be rewritten as

$$\begin{bmatrix}\mathbf{v}_\text{opt}\\ \mathbf{v}_\text{e}\end{bmatrix} = \begin{bmatrix}\mathsf{Y}_{\text{c},1} & \mathsf{O}\\ \mathsf{O} & \mathsf{Y}_{\text{c},2}\end{bmatrix}\begin{bmatrix}\mathsf{B}_1 & \mathsf{B}_2\\ \mathsf{B}_3 & \mathsf{B}_4\end{bmatrix}\begin{bmatrix}\hat{\mathbf{p}}_+\\ \mathbf{0}\end{bmatrix}, \tag{8}$$

where $\hat{\mathbf{p}}_+$ represents the first N_p propagating components of $\mathbf{p}_+$ (the evanescent components of the incident field are assumed to be zero at the output). The unknowns $\hat{\mathbf{p}}_+$ and $\mathbf{v}_\text{e}$ can then be solved as

$$\hat{\mathbf{p}}_+ = \mathsf{B}_1^{-1}\mathsf{Y}_{\text{c},1}^{-1}\mathbf{v}_\text{opt}, \tag{9}$$

$$\mathbf{v}_\text{e} = \mathsf{Y}_{\text{c},2}\mathsf{B}_3\hat{\mathbf{p}}_+. \tag{10}$$

The reflection at the duct end generates evanescent waves, which will cause the synthesized beam to deviate from the theoretical one. Fig. 3 shows good agreement between the theoretical and synthesized directivity factors and beams. A directional beam with a near-planar wavefront can be observed in the near field with regularly distributed sidelobes.

3.2 Point-source array

Next, we present the beam pattern synthesis by an array of point sources, rather than the more theoretical multimodal incident wave. For simplicity, the problem is studied in a bidimensional waveguide. We consider a linear arrangement of point sources located on a transversal line upstream from the opening, far enough to ensure that all the evanescent waves emitted by the sources are negligible at the opening. From the modal representation of the Green's function in the waveguide, we reconstruct $\mathbf{p}_+$ by determining the locations and strengths of N_p point sources:

$$\sum_{m=0}^{N_\text{p}-1} kQ_m \frac{\varphi_n(x_m)}{-2\text{i}k_{z,n}} \text{e}^{\text{i}k_{z,n}|z_\text{s}|} = \hat{p}_{+,n},\ 0 \le n \le N_\text{p} - 1, \tag{11}$$

where $k_{z,n} = \sqrt{k^2 - \gamma_n^2}$ is the axial wavenumber, (x_m, z_s) and Q_m are respectively the coordinates and unknown complex strength of the mth source. We have found that the system is well-conditioned if the sources are equally spaced. The field emitted by the point sources is visualized with the PML-multimodal method [6], as shown in Fig. 4(b). For verification purposes, they have also been validated by the finite element method (FEM) using (x_m, z_s, Q_m) as model inputs.

4. EFFECTS OF EVANESCENT MODES

This section examines the effects of incorporating the evanescent modes into the directivity maximization. We recall the definition of the radiation efficiency of a given velocity distribution $v(x, y)$ on the aperture S [3, 7, 8]:

$$\tau = \frac{W}{\frac{1}{2}\iint\limits_S |v(x,y)|^2 \text{d}S}. \tag{12}$$

The maximization is now solved in a subspace spanned by all propagating modes plus at least one evanescent mode. We have observed a dramatic reduction in the radiation efficiency, accompanied with a rapid increase in the weight of evanescent components even for small N_e. Fig. 5 exemplifies the optimum directivity patterns for a

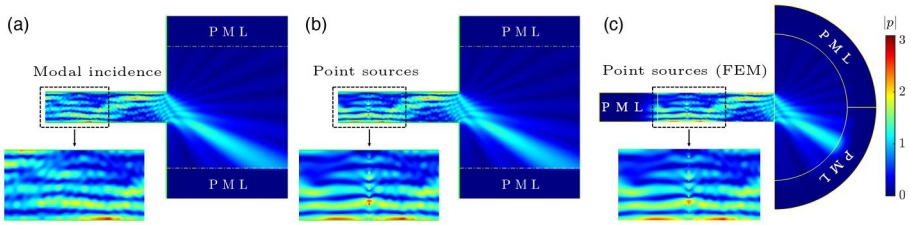

Figure 4. Pressure fields near the aperture for the radiation pattern synthesis. $\theta_\mathrm{d} = 30°$, $k = 30$. (a) Multimodal incidence, $\|\mathbf{p}_+\|$=1. (b) Point sources. (c) FEM validation of (b).

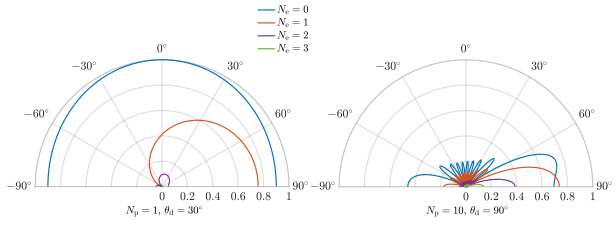

Figure 5. Optimal directivity patterns involving the evanescent modes. $k = 0.5\pi$ and 9.5π.

bidimensional waveguide obtained with $N_\mathrm{e} \leq 3$ (plotted for $\|\mathbf{v}_\mathrm{opt}\| = 1$). As the sound intensity $I_r(r,\theta) \propto |D(\theta)|^2$ at given radial distance and frequency, a decrease in the radiated efficiency is manifested by the "shrinking" of the directivity patterns. Nevertheless, in the extreme case of $\theta_\mathrm{d} = 90°$, for $N_\mathrm{e} = 1$, the assistance of this first evanescent mode (orange line) does not significantly reduce the intensity compared to the pattern for $N_\mathrm{e} = 0$ (blue line) but in turn steers the main lobe precisely into the desired sideline direction. However, the optimal velocity is dominated by its evanescent components with a weight of 0.85. Although its implementation is difficult in hollow waveguides, it could be possible when the waveguide end is filled with structured media through which evanescent modes can be effectively emitted.

5. CONCLUSIONS

A rigorous formulation of the maximum directivity factor for a flanged aperture is proposed, by which an optimal directional beam can be created. It is reasonable to discard the evanescent modes in the maximization process so that the optimum velocity distribution exhibits adequate radiation efficiency and is physically achievable via hollow horns.

6. REFERENCES

[1] R. Pritchard, "Maximum directivity index of a linear point array," *The Journal of The Acoustical Society of America*, vol. 26, no. 6, pp. 1034–1039, 1954.

[2] J. L. Butler and S. L. Ehrlich, "Superdirective spherical radiator," *the Journal of the Acoustical Society of America*, vol. 61, no. 6, pp. 1427–1431, 1977.

[3] E. G. Williams, *Fourier acoustics: sound radiation and nearfield acoustical holography*. Academic press, 1999.

[4] L. Beranek and T. Mellow, *Acoustics: Sound Fields, Transducers and Vibration*. Academic Press, 2019.

[5] R. A. Horn and C. R. Johnson, *Matrix analysis*. Cambridge university press, 2012.

[6] S. Félix, J.-B. Doc, and M. A. Boucher, "Modeling of the multimodal radiation from an open-ended waveguide," *The Journal of the Acoustical Society of America*, vol. 143, no. 6, pp. 3520–3528, 2018.

[7] C. Morfey, "A note on the radiation efficiency of acoustic duct modes," *Journal of Sound and Vibration*, vol. 9, no. 3, pp. 367–372, 1969.

[8] K. A. Cunefare, "The minimum multimodal radiation efficiency of baffled finite beams," *The Journal of the Acoustical Society of America*, vol. 90, no. 5, pp. 2521–2529, 1991.